HHS Public Access

Author manuscript

Cancer Res. Author manuscript; available in PMC 2017 July 01.

Published in final edited form as:

Cancer Res. 2016 July 1; 76(13): 4002–4011. doi:10.1158/0008-5472.CAN-15-3189.

p27 is a Candidate Prognostic Biomarker and Metastatic Promoter in Osteosarcoma

Yiting Li[1,4,5,*], **Manjula Nakka**[1,5,*], **Aaron J. Kelly**[1,3], **Ching C. Lau**[1,3,4,5], **Mark Krailo**[6,7], **Donald A. Barkauskas**[6,7], **John M. Hicks**[2], and **Tsz-Kwong Man**[1,3,4,5,#]

[1]Department of Pediatrics, Baylor College of Medicine, Houston, TX

[2]Department of Pathology, Baylor College of Medicine, Houston, TX

[3]Program of Structural and Computational Biology and Molecular Biophysics, Baylor College of Medicine, Houston, TX

[4]Dan L. Duncan Cancer Center, Baylor College of Medicine, Houston, TX

[5]Texas Children's Hematology and Oncology Centers, Texas Children's Hospital, Houston, TX

[6]Children's Oncology Group, Monrovia, CA

[7]Department of Preventive Medicine, Keck School of Medicine, University of Southern California, Los Angeles, CA

Abstract

Metastatic progression is the major cause of death in osteosarcoma, the most common bone malignancy in children and young adults. However, prognostic biomarkers and efficacious targeted treatments for metastatic disease remain lacking. Using an immunoproteomic approach, we discovered that autoantibodies against the cell cycle kinase inhibitor p27 (KIP1, CDKN1B) were elevated in plasma of high-risk osteosarcoma patients. Using a large cohort of serum samples from osteosarcoma patients (n=233), we validated that a higher level of the p27 autoantibody significantly correlated with poor overall and event-free survival ($p < 0.05$). Immunohistochemical analysis also showed that p27 was mislocalized to the cytoplasm in the majority of osteosarcoma cases and in highly metastatic osteosarcoma cell lines. We demonstrated that ectopic expression of cytoplasmic p27 promoted migration and invasion of osteosarcoma cells, whereas shRNA-mediated gene silencing suppressed these effects. Additionally, mutations at the p27 phosphorylation sites S10 or T198, but not T157, abolished the migratory and invasive

[#]Corresponding author: Tsz-Kwong Man, Associate Professor, Section of Hematology and Oncology, Department of Pediatrics, Baylor College of Medicine, and Texas Children's Cancer and Hematology Centers; Address: 1102 Bates Ave, Houston, Texas 77030-2399; Tel: (832) 824-4682; Fax: (832) 825-4038; ctman@txch.org.

[*]These two authors contributed equally in this study

Disclosure of Potential Conflicts of Interest: The authors disclosed no potential conflicts of interest.

Authors Contribution

Conception and design: TKM

Development of methodology: YL and MN

Acquisition of data (provided animals, acquired and managed patients, provided facilities, etc.): YL, MN, CCL, MK, and DAB

Analysis and interpretation of data (e.g., statistical analysis, biostatistics, computational analysis): YL, MN, AJK, JMH, and TKM

Writing, review, and/or revision of the manuscript: YL, MN, AJK, and TKM

Administrative, technical, or material support (i.e., reporting or organizing data, constructing databases): CCL and TKM

Study supervision: TKM

phenotypes. Furthermore, the development of pulmonary metastases increased in mice injected with cells expressing cytoplasmic p27 compared with an empty vector control. Collectively, our findings support further investigation of p27 as a potential prognostic biomarker and therapeutic target in osteosarcoma cases exhibiting aberrant p27 subcellular localization.

Keywords

osteosarcoma; p27; metastasis; cytoplasmic mislocalization; and prognosis

Introduction

Osteosarcoma (OS) is the most common malignant bone tumor in children. Approximately 400–900 new cases are diagnosed each year in the United States (1). The standard clinical treatment consists of a combination of surgery and chemotherapy. With this regimen, the prognosis of localized OS has improved dramatically when compared to surgery alone (2). The pressing clinical problem, however, is that the prognosis for metastatic, refractory and recurrent OS is still dismal (3). Approximately 20% of OS patients have clinically detectable metastasis at the time of diagnosis (2). Even with current treatment protocols, the progression-free survival rate for patients with metastatic OS is still less than 20%, indicating that the existing regimens are not effective for these patients (4,5). Detection of patients with high metastatic potential or clinical risk early may help to prevent the use of ineffective therapy, which allows extra time for the tumor to develop chemoresistance and metastatic spread. In addition, identification and characterization of key metastatic determinants may lead to the development of new targeting strategies and therapeutic options once the high-risk patients are identified.

A vast amount of literature has indicated that cancer patients often produce autoantibodies to tumor-associated antigens (TAAs) that are overexpressed, modified, or aberrantly cleaved or localized in tumor cells (6). Given that these autoantibodies are considered reporters of the immune response to an early and developing tumor, they are excellent candidate biomarkers for early cancer detection and may lead to identification of potential therapeutic targets. In fact, autoantibodies against TAAs have been shown to be useful in both cancer diagnosis and prognosis (6). Besides being present in peripheral blood, the persistence and stability of autoantibodies in plasma is an added benefit over other potential markers, including TAAs themselves, which are released by tumor cells but are rapidly cleared after circulating in the plasma for a limited amount of time (7). Emerging evidence indicates that many TAAs detected by autoantibodies are important cellular proteins, such as ERBB2, MYC, and TP53, whose aberrant regulation or alteration could be linked to malignancy (8). In this study, we adopted an immunoproteomic approach for identifying important metastatic targets in OS.

Although well-known tumor suppressor genes, such as TP53, RB1 and PTEN, have been implicated in OS (9–11), little is known about p27. p27 or $p27^{kip1}$ (encoded by CDKN1B) is a cyclin-dependent kinase (CDK) inhibitor that negatively regulates cell proliferation through the inhibition of cell cycle progression (12). In a quiescent state, the p27 protein is expressed mainly in the nucleus and binds to the cyclin/CDK complex to inhibit cell cycle

progression. Degradation of the protein is regulated predominantly through the ubiquitin pathway (55). Gene knockout studies have shown that mice lacking p27 develop multi-organ hyperplasia and tumorigenesis (13,14). However, recent data indicate that p27 also has oncogenic properties, which are distinct from the cell cycle regulatory functions (15). In this study, we showed that p27 autoantibody is prognostically significant and the mislocalization of the protein promotes tumor cell migration and invasion as well as metastasis formation in OS.

Materials and Methods

Patients and samples

To identify autoantibodies associated with high-risk in OS, plasma samples from patients who developed localized (n=26) or metastatic disease (n=13) within one year of follow-up, and anonymized patients with noncancerous diseases or no disease (n= 21), i.e. child checkup, flu, constipation, gastroenteritis, or febrile seizure, were analyzed by the ProtoArray and Luminex platforms. These samples were collected at the time of diagnosis from Texas Children's Hospital and other collaborating institutions. Serum samples from OS patients and their survival information were provided by the Children's Oncology Group (COG). All patients gave consent to institutional review board-approved protocols. The clinical information of patients used in this study is summarized in Supplementary Table S1.

Autoantibody profiling analysis

ProtoArray Human Protein Array v4.0 (ThermoFisher Scientific, Waltham, MA) that contains 8,268 proteins was used to detect autoantibodies in the plasma samples according to the manufacturer's instruction. The detailed procedure is described in the Supplementary Methods. The experiments were repeated thrice. Then, the background subtracted intensities of the whole array were quantile-normalized and log-transformed. The threshold of the low intensity values was set at 5. The intensities of the duplicate spots for each protein were averaged and control spots were removed. p-values were calculated by using unpaired, 2-tailed t-test. The selection criteria for high-risk autoantibodies were as follows: (1) $p < 0.001$ in high-risk vs. control and $p < 0.05$ in high-risk vs. low-risk comparisons, and (2) log fold change >=1. The ProtoArray data (GSE78192) were deposited to the Gene Expression Omnibus (GEO) repository.

ProtoPlex immune response assay to measure the p27 autoantibody

The autoantibody validation assays were performed using the ProtoPlex service from ThermoFisher Scientific. The detailed procedure is described in the Supplementary Methods. p27 autoantibody fluorescence intensity values in the COG cohort were background corrected for BSA level, log-transformed, and binarized by median cutoff. Kaplan-Meier analysis was performed to test if a higher level of the p27 autoantibody correlated with poor outcome, and significance was evaluated using a one-tailed version of the log-rank statistic in overall and event-free survival. In event-free survival analysis, events indicated whether death or relapse had occurred in each patient. To ensure p27 was an independent prognostic factor, we confirmed its significance by controlling for the known

prognostic factor, i.e. metastasis at diagnosis, using a multivariate Cox proportional hazard model. For all statistical tests, $p < 0.05$ is considered statistically significant.

Immunohistochemistry

OS cells were cultured on Lab-Tek chamber slides (Nunc, Rochester, NY). After adhesion, cells were fixed with 2% formaldehyde (Sigma-Aldrich) and washed three times with phosphate buffered saline (ThermoFisher Scientific). For tissue microarrays, the arrays were incubated at 60°C for one hour, deparaffinized with xylene, and rehydrated. Antigen retrieval was performed at 95°C for 30 minutes in Antigen Unmasking Solution (Vector Labs, Burlingame, CA). Then, the slides were incubated with 3% hydrogen peroxide and normal horse serum (Vector Labs) for 30 minutes. After that, slides were incubated overnight with mouse anti-human p27 antibody (sc-56338, 1:200, Santa Cruz Biotechnology, Santa Cruz, CA) at 4°C. A biotinylated horse anti-mouse IgG antibody (1:200) and the streptavidin-biotin-peroxidase reaction (Vector Labs) were added sequentially. After color reaction with 3,3-diaminobenzidine solution (Vector Labs), the slides were dehydrated and mounted. The staining results were examined and scored by our pathologist (J.H.) to determine if p27 was expressed in the tumor sections.

Cell Culture

SaOS-2, LM7, Dunn, K7, DLM8 and K7M3, were generously provided by Dr. Eugenie S. Kleinerman from the M.D. Anderson Cancer Center at the University of Texas-Houston. SaOS-2 is a human OS cell line with low metastatic potential (16). The metastatic LM7 cell line was developed by repetitive cycling of SaOS-2 cells through the lungs of nude mice seven times (17). DLM8 and K7M3 are metastatic murine OS cell lines, which were derived from either repeated implantation or injection of Dunn and K7, respectively (18,19). Cells were cultured in Dulbecco's Modified Eagle Medium supplemented with 10% fetal bovine serum (ThermoFisher Scientific) at 37°C in a humidified 5% CO_2 incubator. They were tested to be mycoplasma-free. Identities of the cell lines were validated by STR DNA fingerprinting using the AmpF_STR Identifiler kit according to the manufacturer's instruction (ThermoFisher Scientific).

p27 constructs and transfection

p27 constructs harboring fusions with Nuclear Export Sequence (NES) and enhanced yellow fluorescent protein (EYFP, Clontech, Mountain View, CA) were stably expressed in lowly metastatic SaOS-2 cells. The p27 and control constructs (p27CK-, NES-p27CK- and pEYFP) were kindly provided by Dr. Catherine Denicourt with the University of Texas-Houston. Specifically, NES-p27 was constructed by fusing two NES sequences of protein kinase inhibitor (residues 35–49) in tandem to the NH_2 terminus. The Cyclin–CDK complex binding domain of the p27 construct was mutated (CK-) to control for the cell cycle inhibitory function of p27 (15). The three p27 phosphomutants (NES-p27CK-S10A, -T157A, and -T198A) were generated by replacing serine 10 (S10), threonine 157 (T157), and threonine 198 (T198) on the p27 cDNA with alanine (A) using the QuikChange Lightning Site-Directed Mutagenesis Kit (Stratagene, La Jolla, CA). They were subsequently confirmed by Sanger Sequencing (Supplementary Fig. S1). Transfections were performed using FuGENE 6 Transfection Reagent (Roche Applied Sciences, Indianapolis,

IN). Selection for stable transfectants was started 48 hours after transfection using 1.25 mg/ml Geneticin (ThermoFisher Scientific).

Knockdown of p27 expression in LM7

Two specific MISSION TRC Lentivirus shRNAs for p27 and a shRNA non-target control were used in the silencing experiment (Sigma-Aldrich). 25 μl of each of the p27 shRNA viruses and 16 μg of hexadimethrine bromide (Santa Cruz Biotechnology) were added to each well containing 2 ml of LM7 cells. 1 μg/ml of Puromycin (Sigma-Aldrich) was used for selection at 48 hours after transduction. The sequences for the p27 shRNAs are shown in the Supplementary Methods.

Migration and invasion assays

CytoSelect 24-well Migration and Invasion Assays (Cell Biolabs, San Diego, CA) were used to measure the migratory and invasive capabilities of the p27 mutant and control cells. 3×10^5 cells in serum-depleted medium were added to the upper chamber of a transwell. For the invasion assay, the upper surface of a transwell was coated with dried basement membrane matrix solution. Medium containing 10% fetal bovine serum was added to the lower well. After 6–24 hours of incubation, the migrated and invaded cells were stained by the Cell Stain Solution, which contains crystal violet, and counted in 3–4 fields under a microscope and used for statistical analysis.

Experimental metastasis assay

To measure the metastatic ability of cytoplasmic p27 *in vivo*, we used a tail-vein injection mouse model. 1.5 X 10^6 of SaOS-2 cells containing empty vector or NES-p27CK- as well as metastatic LM7 cells were injected intravenously into the lateral tail vein of 4–6-week-old NOD/SCID mice of both sexes. Five mice were injected in each group. The mice were bred and maintained in a specific pathogen-free animal facility at the Texas Children's Hospital. Mice were euthanized either when they were moribund or six months after the injection of the tumor cells. The lungs of the mice were harvested in 10% formalin, embedded in paraffin and sectioned. The sections were then stained with hematoxylin and eosin, and examined for the occurrence of metastases under a microscope by our pathologist (J.H.). All animal studies were conducted according to institutional animal care and use committee (IACUC) protocols after approval was obtained from our Institutional Review Board.

Data analysis and other methods

Unless stated otherwise, all the statistical comparisons were performed by student unpaired t-tests with $p < 0.05$ were considered significant. Additional details of the methods used are described in the Supplementary Methods.

Results

The p27 autoantibody is elevated in high-risk OS patients

To identify dysregulated proteins in high-risk patients, we first pooled the plasma samples from OS patients, who developed metastasis and localized disease within the first year of

follow-up into a high-risk group and a low-risk group, respectively. Then, the healthy or non-cancerous pediatric patients were pooled into a control group. The pooled sample from each of the three groups was hybridized with a high-density human protein microarray (ProtoArray). The clinical characteristics of the cohort are listed in Supplementary Table S1. Our results showed that six autoantibodies for TCP10, RPS6KB3, MAPK11, CDKN1B, TRPT1 and TFPT showed significantly higher intensities in the high-risk group than those in the low-risk and control groups (Supplementary Table S2). p27 was selected for further investigation and validation, because it is a known tumor suppressor gene that inhibits cell cycle progression (12) (Fig. 1A). Using an orthogonal Luminex xMAP assay, we measured the p27 autoantibody level in individual, rather than pooled, plasma samples. The results show that the p27 autoantibody level was significantly increased in the high-risk group when compared to the low-risk group (Fig. 1B, $p = 0.0134$), suggesting that it carries a prognostic value. Of note, a subset of patients had a much higher level of the p27 autoantibody within the high-risk group.

The p27 autoantibody predicts overall survival

Since the autoantibody was elevated in the high-risk patients, we further hypothesized that a higher level of the autoantibody predicts a worse outcome in OS patients. To test this, we used the Luminex xMAP assay to measure the amounts of the p27 autoantibody in a large OS cohort (n=233) obtained from COG. Using the median abundance as a cutoff, a higher p27 autoantibody level was significantly associated with poor overall ($p = 0.033$, HR = 1.46) and event-free (p = 0.0079, HR = 1.57) survival of OS patients (Fig. 2). Patients with a low level of the p27 autoantibody had a 5-year overall survival rate of 67% (95% CI, 59% to 77%) and 5-year event-free survival of 57% (95% CI, 48% to 67%), whereas patients with a high level of p27 autoantibody had a 5-year overall survival rate of 52% (95% CI, 44% to 62%) and 5-year event-free survival of 40% (95% CI, 31% to 50%). After controlling for the known prognostic factor at diagnosis, i.e. initial metastasis or metastasis at diagnosis, we found that the associations of the p27 autoantibody with overall and event-free survival remained significant ($p < 0.05$). When stratified by initial metastasis, p27 autoantibody levels did not significantly correlate with overall or event-free survival (Overall: $p = 0.27$, HR = 1.21; Event-free: $p = 0.18$, HR = 1.29) in cases with initial metastasis; whereas in patients with no detectable metastasis at diagnosis, a high p27 level significantly correlated with poor outcome in both overall and event-free survival (Overall: $p = 0.04$, HR = 1.63; Event-free: $p = 0.013$, HR = 1.73) (Fig 2). These results indicate that the p27 autoantibody may help to identify patients who currently would be classified as “low risk” because of their localized disease status, but actually have significantly worse survival rates.

Cytoplasmic mislocalization of p27 in OS tissues and metastatic cell lines

To examine if p27 is dysregulated in OS, we performed p27 immunohistochemistry on two OS tissue microarrays (TMAs). One was from the Children’s Oncology Group (COG) and the other was from a commercial source (US BioMax). Our results showed that 82% of OS cores showed either strong (30%) or weak (52%) cytoplasmic staining of p27 in the COG TMA. Similarly, 80% of OS cores had cytoplasmic staining of p27, in which 26 cases (52%) showed strong expressions and 14 cases (28%) showed weak expression in the US BioMax TMA (Fig. 3A and B). No nuclear expression of p27 was observed in both TMAs. These

staining results suggest that p27 was expressed but mislocalized in the cytoplasm of the majority of OS cases. Since cytoplasmic mislocalization of p27 has been implicated in metastasis of other solid tumors (15,20), we performed p27 immunohistochemistry on three pairs of isogenic OS metastatic cell lines. As shown in Fig. 3C, p27 expression was either very low or restricted in nucleus in the lowly metastatic parental cell lines (SaOS-2, K7, DUNN). However, p27 was expressed relatively stronger in the cytoplasm of all three metastatic sublines (LM7, K7M3, DLM8). These cell line results suggest that cytoplasmic expression of p27 may be linked to metastatic properties of OS cells.

Cytoplasmic p27 promotes the metastatic potential of OS cells *in vitro*

To test if cytoplasmic mislocalization of p27 can increase the metastatic potential of OS cells, a p27 construct harboring a fusion with a Nuclear Export Sequence (NES) and enhanced yellow fluorescent protein (EYFP) was stably expressed in the lowly metastatic SaOS-2 cell line with low cytoplasmic p27 expression. The Cyclin–CDK complex binding domain of the p27 construct was mutated (CK-) to control for the cell cycle inhibitory function of p27 (Fig. 4A). In the stable cell line containing the empty vector control (pEYFP), the fluorescent protein was expressed in both nucleus and cytoplasm of the tumor cell (Fig. 4B). In contrast, p27 was expressed in the cytoplasm of the cells harboring NES-p27CK- (Fig. 4B). To examine the effect of cytoplasmic p27, *in vitro* migration and invasion assays were performed on the NES-p27 CK-mutant and controls. As shown in Fig. 4C, ectopic expression of cytoplasmic p27 significantly increased the numbers of migrated and invaded cells relative to the empty vector control ($p = 2 \times 10^{-7}$ for migration and $p = 2 \times 10^{-4}$ for invasion). Similar results were observed in the repeated experiment (Supplementary Figure S2). The results suggest that cytoplasmic mislocalization of p27 was sufficient to promote the motility and invasiveness of OS cells. The migratory and invasive abilities of NES-p27 cells without the CK mutation behaved similarly to the CK- mutant, suggesting that the pro-metastatic effect of cytoplasmic p27 is not associated with its cyclin-CDK inhibitory function (Supplementary Figure S3).

The effect of phosphorylation on the pro-migration/invasion function of cytoplasmic p27

Phosphorylation plays an important role in regulating the protein activity and subcellular location of p27 (21–23). To test if p27 phosphorylation has any effects on the pro-migration/invasion function of p27 when it is localized in the cytoplasm of OS, we created three stably transfected mutants harboring an alanine mutation in each of the three major phosphorylation sites, namely S10, T157, and T198, on the NES-p27CK- construct (Fig. 4A). Evidence that these mutated phosphoproteins were cytoplasmically localized are shown in Fig. 4B. The transwell assay showed that both S10A and T198A mutations abolished the promoting effect of NES-p27CK- on cell migration and invasion, while the migratory or invasive abilities of the T157A mutant were similar to the controls (Fig. 4C). The growth rates of NES-p27CK- and all phosphomutants were similar to the control cells, suggesting the changes of metastatic potential in the NES-p27CK- cells and the phosphomutants were not due to differences in growth rates (Supplementary Figure S4). These results indicate that the S10 and T198 phosphorylations are not just important for subcellular localization of p27, but are also critical for the pro-metastatic function of cytoplasmic p27 in OS cells.

To investigate the pro-metastatic mechanism of cytoplasmic p27, we examined RHOA-GTPase activity, which has been reported to be a downstream effector protein of cytoplasmic p27 for cell motility in other tumors (22,24). As shown in Fig. 4D, the RHOA activity, as measured by the level of GTP-bound RHOA, decreased significantly in NES-p27CK- cells compared to that in the empty vector control. Among the three phosphomutants, we found that the S10A mutation restored the RHOA activity, which could explain the observation that the cell motility was lower in this mutant. As expected from the transwell assays, the RHOA activity of the T157 mutant was similar to that in the NES-p27CK- cells. Interestingly, despite the decrease of cell migration and invasion in the T198A mutant, it showed little inhibitory effect on the RHOA activity (Fig. 4D).

Knockdown of p27 decreases cell migration and invasion and restores RHOA activity

Next, we tested if cytoplasmic p27 was necessary for the pro-metastatic effect. Two shRNAs targeting p27 were stably transduced to highly metastatic LM7 cells that express cytoplasmic p27 (Fig. 3C). The p27 mRNA levels were significantly reduced in the shRNA-1 and shRNA-2 cells compared to the parental LM7 cells and LM7 cells with control shRNAs ($p < 0.05$, Fig. 5A). The growth rates of the two p27-silenced mutants were significantly higher than the scramble and parental controls ($p < 0.05$, Fig. 5B). Transwell migration and invasion assays showed that cell motility and invasiveness of the p27-shRNA mutants were significantly lower than those in the scramble control ($p < 0.05$, Fig. 5C). Similar results were observed in a repeated experiment and using a 2-D migration assay (Supplementary Figures 5 and 6). Furthermore, the RHOA activities of the p27-silenced mutants were higher than those in the controls (Fig. 5D). Taken together, the results of the NES and shRNA mutants showed that cytoplasmic p27 was both sufficient and necessary for promoting cell motility and invasiveness of OS cells *in vitro*. However, the exact mechanism of how various p27 phosphorylations affect this phenotype still needs further investigation.

p27 mislocalization increases the formation of lung metastases in an animal model

To confirm cytoplasmic p27 can promote the development of metastasis, we injected SaOS-2 cells containing NES-p27CK- into NOD/SCID deficient mice via lateral tail vein. SaOS-2 cells with empty vector and LM7 cells were used as negative and positive controls, respectively. The result showed that only 1 out of 5 mice injected with cells containing the empty vector developed lung metastasis, while 3 out of 5 mice and 4 out of 5 mice developed lung metastases after injection with cells containing NES-p27CK- and highly metastatic LM7 cells, respectively (Fig. 6A). In addition, the total number of lung metastases in mice injected with the NES-p27CK- cells was significantly higher than the controls ($p < 0.05$, Fig. 6A). The metastatic lung nodules in the mice with NES-p27CK- and LM7 cells were visible macroscopically (Fig. 6B) and were confirmed under the microscope by our pathologist (Fig. 6C). Additional images of other lung metastases are shown in Supplementary Figure S7. These results indicate that cytoplasmic p27 is sufficient to generate a higher number of lung metastasis *in vivo,* likely by increasing the motility and invasiveness of the tumor cells.

Discussion

Identifying prognostic biomarkers and therapeutic targets for OS has been a difficult task and a major obstacle in the field. The reason, in part, is due to the highly rearranged genomes that occur in OS. Despite intensive studies from various groups, identifying potential biomarkers and targets from the genomic space has not significantly improved the clinical outcomes of OS patients (25–28). In this study, we showed that higher levels of p27 autoantibody significantly correlated with both poor overall and event-free survival. Most interestingly, patients with localized disease at diagnosis but high p27 autoantibody levels had poor overall and event-free survival. This suggests that the p27 autoantibody may be useful in detecting a subset of either localized patients with a higher clinical risk or patients with micrometastases too small to be detected by conventional imaging techniques at diagnosis. These patients, together with metastatic patients, could be treated more aggressively or with an alternative approach to improve their outcomes.

Previous studies have shown that many different human cancers exhibit reduced levels of p27 proteins (29–35). Furthermore, cytoplasmic mislocalization of p27 has been shown in a number of human tumors, which include esophageal carcinomas (36), colorectal carcinoma (37), invasive and metastatic melanomas (15) and breast carcinomas (36,38,39). AKT1 activation with p27 mislocalization was observed in approximately 40% of primary breast cancers (21,38,40). Prognostically, cytoplasmic p27 was associated with poor survival and predicts poor prognosis in breast carcinomas (21), acute myelogenous leukemia (41), pancreatic cancer (42) and ovarian carcinomas (43). Our TMA results show that a major proportion of OS patients had cytoplasmic mislocalization of p27, indicating that they may have a higher metastatic potential at diagnosis. The variation in the percentage of cases with high and low staining of cytoplasmic p27 between the two TMAs may be due to differences in fixation and decalcification procedures used in preparing the TMAs. Nonetheless, the large proportion of cases with p27 mislocalization (both low and high staining) fit very well with historic data that a large proportion of OS patients develop metastatic disease when only surgery is used (2). One of our future goals is to examine if p27 degradation or mislocalization in OS confers a poorer outcome in OS using clinically annotated cases.

Although p27 dysregulation has been described in osteoblast cells and OS, little is known about its role in metastasis (44,45). The discovery of p27 as a tumor-associated antigen in high-risk OS is a novel finding. Our result shows for the first time that cytoplasmic mislocalization of p27 is sufficient and necessary for promoting metastatic potential in OS. Additionally, the p27 shRNAs reduced both nuclear and cytoplasmic expressions of p27 in LM7. We believe that the increase of cell growth in the shRNA mutants was due to decreased nuclear expression of p27, while the decrease of cell motility and invasiveness was due to the decreased cytoplasmic expression of p27. We have further shown that OS cells harboring cytoplasmic p27 increase the occurrence of pulmonary metastases in a mouse model, suggesting that the increase of migration and invasion *in vitro* confer the development of metastasis *in vivo*. Mechanistically, we demonstrated that the increase in cell motility and invasiveness is related to the decrease of RHOA-GTPase activity. These results are consistent with previous findings that p27 mislocalization can promote cell motility in different cell types and metastasis in melanoma (15,24,46,47). Thus, cytoplasmic p27

acquires oncogenic functions that are independent of cell cycle regulation, potentially through effects on RHOA, in OS and other cancers.

Three phosphosites were selected for mutation analysis to understand their contributions to the pro-metastatic phenotype of mislocalized p27. The S10 residue, which is phosphorylated by human kinase-interacting stathmin (hKIS) and other kinases, is known to control p27 nuclear export, XPO1 binding and protein degradation (23). The T157 residue, which is phosphorylated by SGK1 and AKT1 is known to impair nuclear import, affect cytoplasmic localization and increase cyclin D1-CDK4-p27 complex formation (48). On the other hand, the T198 residue can be phosphorylated by RPS6KA1 and AKT1. This residue can affect cytoplasmic localization of the protein and protein stability (22). However, the functions of these phosphosites in relation to the cytoplasmic metastatic function of p27 are largely unknown. Our results indicate that the S10A or T198A mutation can decrease the cell motility and invasiveness of the tumor cells harboring cytoplasmic p27. These results suggest that targeting S10 or T198 phosphorylation may provide a new therapeutic approach for metastatic OS cells harboring cytoplasmic p27. Our results also suggest that the effects of S10A and T198A mutations on RHOA are not the same. The S10 mutation increased RHOA-GTPase activity, while the T198A mutation had no effect on RHOA. The mutation of T198A may affect a downstream player of the RHOA pathway or a RHOA-independent metastatic pathway, such as Rac (49). However, the T198 mutation has been shown to affect RHOA binding and activity in breast cancer cells (22), suggesting that these phosphorylation sites on mislocalized p27 may have cell-type specific effects. This notion is supported by previous studies of fibrosarcoma and trophoblast cells, where cytoplasmic p27 inhibits migration by binding to stathmin (50,51). Further investigations of the function of mislocalized p27 in different tumor types may shed light on this issue. In addition, since human kinase interacting stathmin (hKIS) is known to phosphorylate the S10 residue of p27, identifying a small molecule to inhibit hKIS may provide a new therapeutic targeting strategy for metastatic OS. Development of such a targeting strategy for cytoplasmic p27 will likely to have a widespread application in cancer research.

Although the relationship between the p27 autoantibody levels and the p27 mislocalization in tumor cells is still not known, our study has provided a solid foundation for future association studies between the p27 autoantibody and the subcellular localization of the protein in OS or other cancers. Since we did not observe any cell surface expression of p27 in our experiment, the immunoreactivity of p27 may be due to leakage into bloodstream during tumor lysis and/or necrosis, which is then recognized by the humoral immunity to produce an increase amount of the p27 autoantibody. Further characterization of the p27 mislocalization process will help us to understand how the body’s immune system reacts to the protein, which may provide a new angle for immunotherapy in OS. In summary, our results suggest that further studies of the role of p27 in OS may lead to a better prognostication method at diagnosis, so that high-risk OS patients can be treated more appropriately to improve their chance of survival. Our study also suggests that development of a novel targeted therapy approach, such as inhibition of phosphorylation of the S10 residue, may provide an effective and rational treatment for patients who harbor the p27 mislocalization in the tumor.

Supplementary Material

Refer to Web version on PubMed Central for supplementary material.

Acknowledgments

Financial Support: This work was partly supported by the Multi-Investigator Research Award (RP101335-P02/RP140022-P2) and Baylor College of Medicine Comprehensive Cancer Training Program (RP140102) by Cancer Prevention and Research Institute of Texas, Bear Necessities Pediatric Cancer Foundation, and National Institute of Children's Health and Development (R01 HD074553). The research is also supported by the Chair's Grant U10 CA98543 and Human Specimen Banking Grant U24 CA114766 of the Children's Oncology Group from the National Cancer Institute, National Institutes of Health, Bethesda, MD, USA, and the WWWW (QuadW) Foundation, Inc. (www.QuadW.org). Additional support by the National Cancer Institute Cancer Center Support Grant (P30CA125123) of the Proteomics Shared Resource at Baylor College of Medicine.

We are thankful to the Bone Sarcoma Committee with COG for their support of this study. We are also grateful to Dr. Shixia Huang and Myra Costello with the Proteomics Shared Resource at Baylor College of Medicine for scanning the ProtoArrays. We thank Drs. Nancy Weigel and Neha Parikh for their technical assistance, and Dr. Xiao-Nan Li for help in the animal study. We are in debt of Drs. Lisa Wang, Lazlo Perlaky, Jeffery Murray and William Myers for their assistance in collecting the plasma samples as well as Carolyn Pena for proofreading the manuscript.

References

1. Chou AJ, Geller DS, Gorlick R. Therapy for osteosarcoma: where do we go from here? Paediatr Drugs. 2008; 10(5):315–27. [PubMed: 18754698]
2. Link, MP.; Eilber, F. Osteosarcoma. In: Eilber, F.; Poplack, D., editors. Principles and Practice of Pediatric Oncology. 3. Philadelphia: Lippincott-Raven Publishers; 1997. p. 889-920.
3. Bielack SS, Kempf-Bielack B, Delling G, Exner GU, Flege S, Helmke K, et al. Prognostic factors in high-grade osteosarcoma of the extremities or trunk: an analysis of 1,702 patients treated on neoadjuvant cooperative osteosarcoma study group protocols. J Clin Oncol. 2002; 20(3):776–90. [PubMed: 11821461]
4. Kager L, Zoubek A, Potschger U, Kastner U, Flege S, Kempf-Bielack B, et al. Primary metastatic osteosarcoma: presentation and outcome of patients treated on neoadjuvant Cooperative Osteosarcoma Study Group protocols. J Clin Oncol. 2003; 21(10):2011–18. [PubMed: 12743156]
5. Bacci G, Briccoli A, Rocca M, Ferrari S, Donati D, Longhi A, et al. Neoadjuvant chemotherapy for osteosarcoma of the extremities with metastases at presentation: recent experience at the Rizzoli Institute in 57 patients treated with cisplatin, doxorubicin, and a high dose of methotrexate and ifosfamide. Ann Oncol. 2003; 14(7):1126–34. [PubMed: 12853357]
6. Wang X, Yu J, Sreekumar A, Varambally S, Shen R, Giacherio D, et al. Autoantibody signatures in prostate cancer. N Engl J Med. 2005; 353(12):1224–35. [PubMed: 16177248]
7. Anderson KS, LaBaer J. The sentinel within: exploiting the immune system for cancer biomarkers. J Proteome Res. 2005; 4(4):1123–33. [PubMed: 16083262]
8. Casiano CA, Mediavilla-Varela M, Tan EM. Tumor-associated antigen arrays for the serological diagnosis of cancer. Mol Cell Proteomics. 2006; 5(10):1745–59. [PubMed: 16733262]
9. Malkin D, Li FP, Strong LC, Fraumeni JF Jr, Nelson CE, Kim DH, et al. Germ line p53 mutations in a familial syndrome of breast cancer, sarcomas, and other neoplasms. Science. 1990; 250(4985):1233–38. [PubMed: 1978757]
10. Toguchida J, Ishizaki K, Sasaki MS, Nakamura Y, Ikenaga M, Kato M, et al. Preferential mutation of paternally derived RB gene as the initial event in sporadic osteosarcoma. Nature. 1989; 338(6211):156–58. [PubMed: 2918936]
11. Freeman SS, Allen SW, Ganti R, Wu J, Ma J, Su X, et al. Copy number gains in EGFR and copy number losses in PTEN are common events in osteosarcoma tumors. Cancer. 2008; 113(6):1453–61. [PubMed: 18704985]
12. Toyoshima H, Hunter T. p27, a novel inhibitor of G1 cyclin-Cdk protein kinase activity, is related to p21. Cell. 1994; 78(1):67–74. [PubMed: 8033213]

13. Fero ML, Rivkin M, Tasch M, Porter P, Carow CE, Firpo E, et al. A syndrome of multiorgan hyperplasia with features of gigantism, tumorigenesis, and female sterility in p27(Kip1)-deficient mice. Cell. 1996; 85(5):733–44. [PubMed: 8646781]
14. Kiyokawa H, Kineman RD, Manova-Todorova KO, Soares VC, Hoffman ES, Ono M, et al. Enhanced growth of mice lacking the cyclin-dependent kinase inhibitor function of p27(Kip1). Cell. 1996; 85(5):721–32. [PubMed: 8646780]
15. Denicourt C, Saenz CC, Datnow B, Cui XS, Dowdy SF. Relocalized p27Kip1 tumor suppressor functions as a cytoplasmic metastatic oncogene in melanoma. Cancer Res. 2007; 67(19):9238–43. [PubMed: 17909030]
16. Fogh J, Fogh JM, Orfeo T. One hundred and twenty-seven cultured human tumor cell lines producing tumors in nude mice. J Natl Cancer Inst. 1977; 59(1):221–26. [PubMed: 327080]
17. Jia SF, Worth LL, Kleinerman ES. A nude mouse model of human osteosarcoma lung metastases for evaluating new therapeutic strategies. Clin Exp Metastasis. 1999; 17(6):501–06. [PubMed: 10763916]
18. Asai T, Ueda T, Itoh K, Yoshioka K, Aoki Y, Mori S, et al. Establishment and characterization of a murine osteosarcoma cell line (LM8) with high metastatic potential to the lung. Int J Cancer. 1998; 76(3):418–22. [PubMed: 9579581]
19. Khanna C, Prehn J, Yeung C, Caylor J, Tsokos M, Helman L. An orthotopic model of murine osteosarcoma with clonally related variants differing in pulmonary metastatic potential. Clin Exp Metastasis. 2000; 18(3):261–71. [PubMed: 11315100]
20. Wang D, He F, Zhang L, Zhang F, Wang Q, Qian X, et al. The role of p27(Kip1) phosphorylation at serine 10 in the migration of malignant glioma cells in vitro. Neoplasma. 2011; 58(1):65–73. [PubMed: 21067268]
21. Liang J, Zubovitz J, Petrocelli T, Kotchetkov R, Connor MK, Han K, et al. PKB/Akt phosphorylates p27, impairs nuclear import of p27 and opposes p27-mediated G1 arrest. Nat Med. 2002; 8(10):1153–60. [PubMed: 12244302]
22. Larrea MD, Hong F, Wander SA, da Silva TG, Helfman D, Lannigan D, et al. RSK1 drives p27Kip1 phosphorylation at T198 to promote RhoA inhibition and increase cell motility. Proc Natl Acad Sci USA. 2009; 106(23):9268–73. [PubMed: 19470470]
23. Boehm M, Yoshimoto T, Crook MF, Nallamshetty S, True A, Nabel GJ, et al. A growth factor-dependent nuclear kinase phosphorylates p27(Kip1) and regulates cell cycle progression. EMBO J. 2002; 21(13):3390–401. [PubMed: 12093740]
24. Wu FY, Wang SE, Sanders ME, Shin I, Rojo F, Baselga J, et al. Reduction of cytosolic p27(Kip1) inhibits cancer cell motility, survival, and tumorigenicity. Cancer Res. 2006; 66(4):2162–72. [PubMed: 16489017]
25. Wan X, Mendoza A, Khanna C, Helman LJ. Rapamycin inhibits ezrin-mediated metastatic behavior in a murine model of osteosarcoma. Cancer Res. 2005; 65(6):2406–11. [PubMed: 15781656]
26. Demetri GD, Chawla SP, Ray-Coquard I, Le CA, Staddon AP, Milhem MM, et al. Results of an international randomized phase III trial of the mammalian target of rapamycin inhibitor ridaforolimus versus placebo to control metastatic sarcomas in patients after benefit from prior chemotherapy. J Clin Oncol. 2013; 31(19):2485–92. [PubMed: 23715582]
27. Chen X, Bahrami A, Pappo A, Easton J, Dalton J, Hedlund E, et al. Recurrent somatic structural variations contribute to tumorigenesis in pediatric osteosarcoma. Cell Rep. 2014; 7(1):104–12. [PubMed: 24703847]
28. Perry JA, Kiezun A, Tonzi P, Van Allen EM, Carter SL, Baca SC, et al. Complementary genomic approaches highlight the PI3K/mTOR pathway as a common vulnerability in osteosarcoma. Proc Natl Acad Sci USA. 2014; 111(51):E5564–E73. [PubMed: 25512523]
29. Chu IM, Hengst L, Slingerland JM. The Cdk inhibitor p27 in human cancer: prognostic potential and relevance to anticancer therapy. Nat Rev Cancer. 2008; 8(4):253–67. [PubMed: 18354415]
30. Catzavelos C, Bhattacharya N, Ung YC, Wilson JA, Roncari L, Sandhu C, et al. Decreased levels of the cell-cycle inhibitor p27Kip1 protein: prognostic implications in primary breast cancer. Nat Med. 1997; 3(2):227–30. [PubMed: 9018244]

31. Tsihlias J, Kapusta L, Slingerland J. The prognostic significance of altered cyclin-dependent kinase inhibitors in human cancer. Annu Rev Med. 1999; 50:401–23. [PubMed: 10073286]
32. Loda M, Cukor B, Tam SW, Lavin P, Fiorentino M, Draetta GF, et al. Increased proteasome-dependent degradation of the cyclin-dependent kinase inhibitor p27 in aggressive colorectal carcinomas. Nat Med. 1997; 3(2):231–34. [PubMed: 9018245]
33. Catzavelos C, Tsao MS, DeBoer G, Bhattacharya N, Shepherd FA, Slingerland JM. Reduced expression of the cell cycle inhibitor p27Kip1 in non-small cell lung carcinoma: a prognostic factor independent of Ras. Cancer Res. 1999; 59(3):684–88. [PubMed: 9973218]
34. Chiarle R, Budel LM, Skolnik J, Frizzera G, Chilosi M, Corato A, et al. Increased proteasome degradation of cyclin-dependent kinase inhibitor p27 is associated with a decreased overall survival in mantle cell lymphoma. Blood. 2000; 95(2):619–26. [PubMed: 10627471]
35. Piva R, Cancelli I, Cavalla P, Bortolotto S, Dominguez J, Draetta GF, et al. Proteasome-dependent degradation of p27/kip1 in gliomas. J Neuropathol Exp Neurol. 1999; 58(7):691–96. [PubMed: 10411338]
36. Singh SP, Lipman J, Goldman H, Ellis FH Jr, Aizenman L, Cangi MG, et al. Loss or altered subcellular localization of p27 in Barrett's associated adenocarcinoma. Cancer Res. 1998; 58(8): 1730–35. [PubMed: 9563491]
37. Ciaparrone M, Yamamoto H, Yao Y, Sgambato A, Cattoretti G, Tomita N, et al. Localization and expression of p27KIP1 in multistage colorectal carcinogenesis. Cancer Res. 1998; 58(1):114–22. [PubMed: 9426067]
38. Viglietto G, Motti ML, Bruni P, Melillo RM, D'Alessio A, Califano D, et al. Cytoplasmic relocalization and inhibition of the cyclin-dependent kinase inhibitor p27(Kip1) by PKB/Akt-mediated phosphorylation in breast cancer. Nat Med. 2002; 8(10):1136–44. [PubMed: 12244303]
39. Motti ML, De MC, Califano D, Fusco A, Viglietto G. Akt-dependent T198 phosphorylation of cyclin-dependent kinase inhibitor p27kip1 in breast cancer. Cell Cycle. 2004; 3(8):1074–80. [PubMed: 15280662]
40. Shin I, Yakes FM, Rojo F, Shin NY, Bakin AV, Baselga J, et al. PKB/Akt mediates cell-cycle progression by phosphorylation of p27(Kip1) at threonine 157 and modulation of its cellular localization. Nat Med. 2002; 8(10):1145–52. [PubMed: 12244301]
41. Min YH, Cheong JW, Kim JY, Eom JI, Lee ST, Hahn JS, et al. Cytoplasmic mislocalization of p27Kip1 protein is associated with constitutive phosphorylation of Akt or protein kinase B and poor prognosis in acute myelogenous leukemia. Cancer Res. 2004; 64(15):5225–31. [PubMed: 15289327]
42. Fukumoto A, Ikeda N, Sho M, Tomoda K, Kanehiro H, Hisanaga M, et al. Prognostic significance of localized p27Kip1 and potential role of Jab1/CSN5 in pancreatic cancer. Oncol Rep. 2004; 11(2):277–84. [PubMed: 14719054]
43. Rosen DG, Yang G, Cai KQ, Bast RC Jr, Gershenson DM, Silva EG, et al. Subcellular localization of p27kip1 expression predicts poor prognosis in human ovarian cancer. Clin Cancer Res. 2005; 11(2 Pt 1):632–37. [PubMed: 15701850]
44. Drissi H, Hushka D, Aslam F, Nguyen Q, Buffone E, Koff A, et al. The cell cycle regulator p27kip1 contributes to growth and differentiation of osteoblasts. Cancer Res. 1999; 59(15):3705–11. [PubMed: 10446985]
45. Thomas DM, Johnson SA, Sims NA, Trivett MK, Slavin JL, Rubin BP, et al. Terminal osteoblast differentiation, mediated by runx2 and p27KIP1, is disrupted in osteosarcoma. J Cell Biol. 2004; 167(5):925–34. [PubMed: 15583032]
46. Besson A, Gurian-West M, Schmidt A, Hall A, Roberts JM. p27Kip1 modulates cell migration through the regulation of RhoA activation. Genes Dev. 2004; 18(8):862–76. [PubMed: 15078817]
47. Nagahara H, Vocero-Akbani AM, Snyder EL, Ho A, Latham DG, Lissy NA, et al. Transduction of full-length TAT fusion proteins into mammalian cells: TAT-p27Kip1 induces cell migration. Nat Med. 1998; 4(12):1449–52. [PubMed: 9846587]
48. Larrea MD, Liang J, Da ST, Hong F, Shao SH, Han K, et al. Phosphorylation of p27Kip1 regulates assembly and activation of cyclin D1-Cdk4. Mol Cell Biol. 2008; 28(20):6462–72. [PubMed: 18710949]

49. McAllister SS, Becker-Hapak M, Pintucci G, Pagano M, Dowdy SF. Novel p27(kip1) C-terminal scatter domain mediates Rac-dependent cell migration independent of cell cycle arrest functions. Mol Cell Biol. 2003; 23(1):216–28. [PubMed: 12482975]

50. Baldassarre G, Belletti B, Nicoloso MS, Schiappacassi M, Vecchione A, Spessotto P, et al. p27(Kip1)-stathmin interaction influences sarcoma cell migration and invasion. Cancer Cell. 2005; 7(1):51–63. [PubMed: 15652749]

51. Nadeem L, Brkic J, Chen YF, Bui T, Munir S, Peng C. Cytoplasmic mislocalization of p27 and CDK2 mediates the anti-migratory and anti-proliferative effects of Nodal in human trophoblast cells. J Cell Sci. 2013; 126(Pt 2):445–53. [PubMed: 23230143]

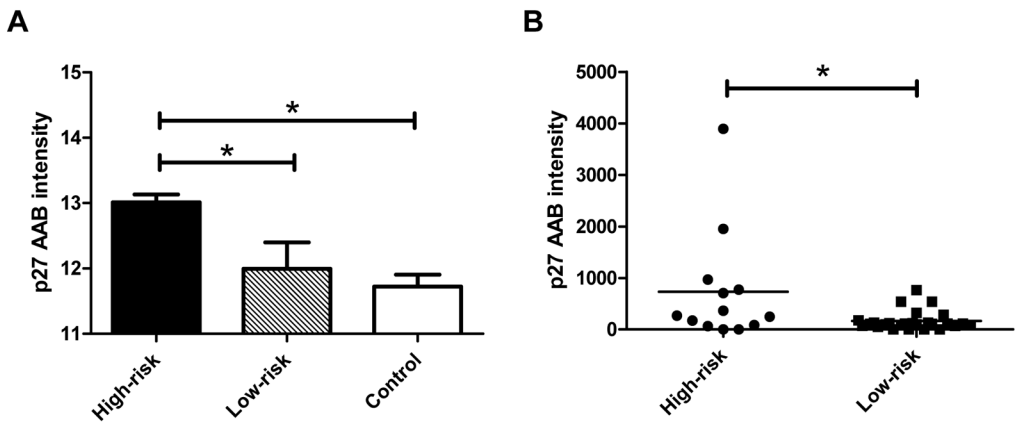

Figure 1.

Identification of p27 as a tumor-associated antigen in high-risk OS. A: The normalized log fluorescent intensity of the p27 autoantibody in the pooled high-risk samples was significantly higher than those in the pooled samples from low-risk and noncancerous diseases ($p < 0.05$) using ProtoArrays. B: The Luminex xMAP assay validated that the p27 autoantibody levels in the individual samples of the high-risk group were significantly higher those in the low-risk group ($p = 0.0134$). The lines in the plot denote the average intensity values of the groups.

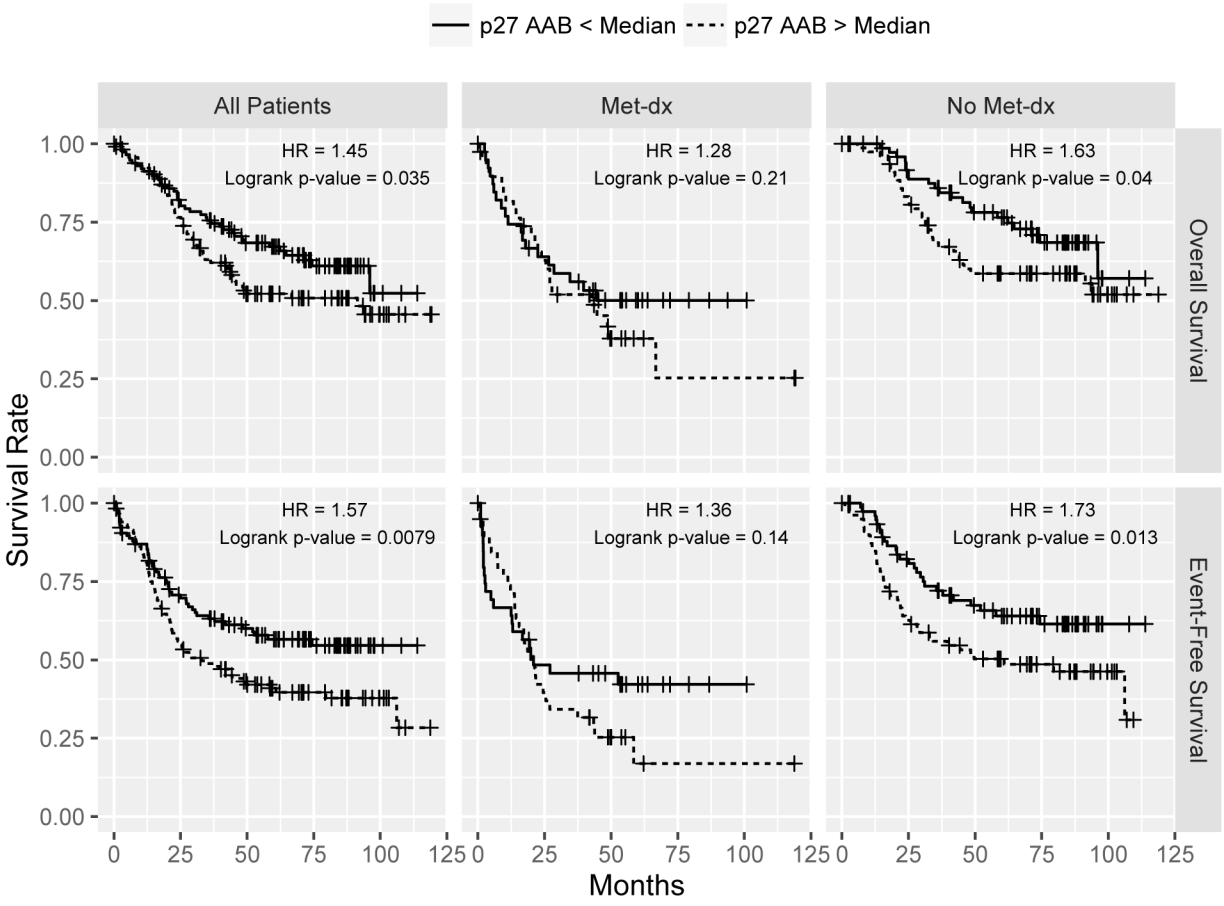

Figure 2.

The Kaplan-Meier curves of the Luminex xMAP assay of the p27 autoantibody in 233 OS serum samples. Using a median intensity cutoff, a higher level of the p27 autoantibody significantly correlated with the poor overall survival (top) and event-free survival (bottom) of the OS patients (left panel). The middle and the right panels show the Kaplan-Meier curves when stratified by the initial metastasis status.

A

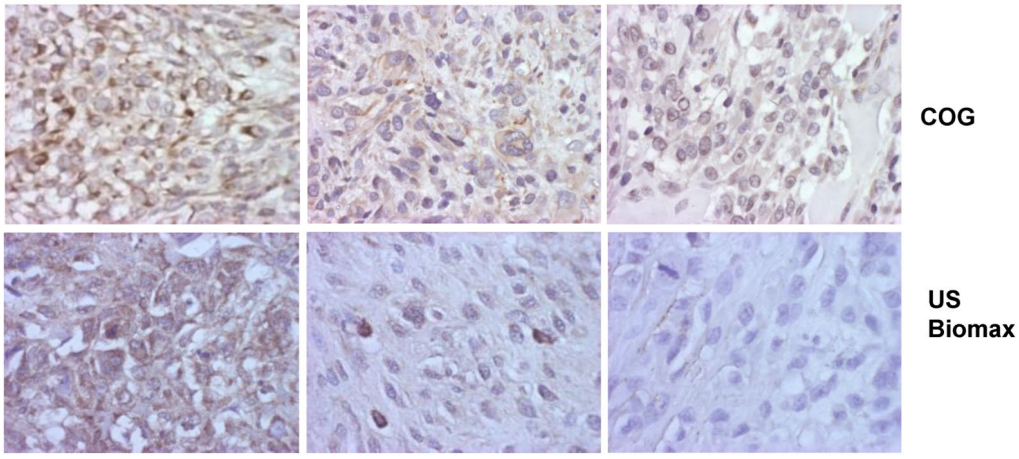

B

Site of stain	IHC Score	Osteosarcoma COG TMA		Osteosarcoma US Biomax TMA	
		Number	%	Number	%
Trace / Negative		11	18	10	20
Cytoplasmic Stain	1-4 (Weak)	33	52	14	28
	5-7 (Strong)	19	30	26	52
Total		63	100	50	100

C

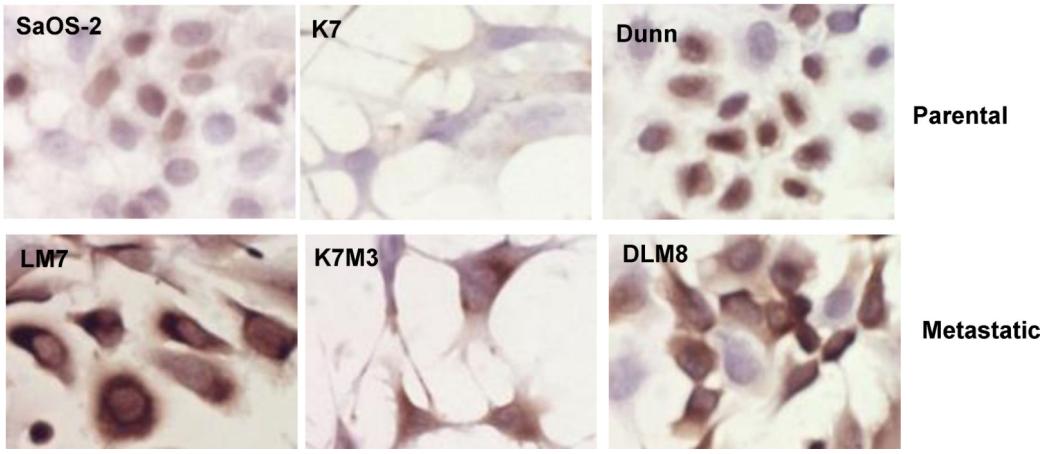

Figure 3.

The p27 protein exhibits cytoplasmic localization in OS cases and metastatic cell lines. A: 10X immunohistochemistry images of p27 staining in two OS tumor tissue microarrays (COG: Children's Oncology Group and US BioMax). B: A table to show the number and % of nuclear and cytoplasmic staining results in the tissue microarrays. C: 40X immunocytochemistry images show that p27 was expressed higher in the cytoplasm of the three OS metastatic cell lines (LM7, K7M3 and DLM8) when compared to the parental cells (SaOS-2, K7 and Dunn).

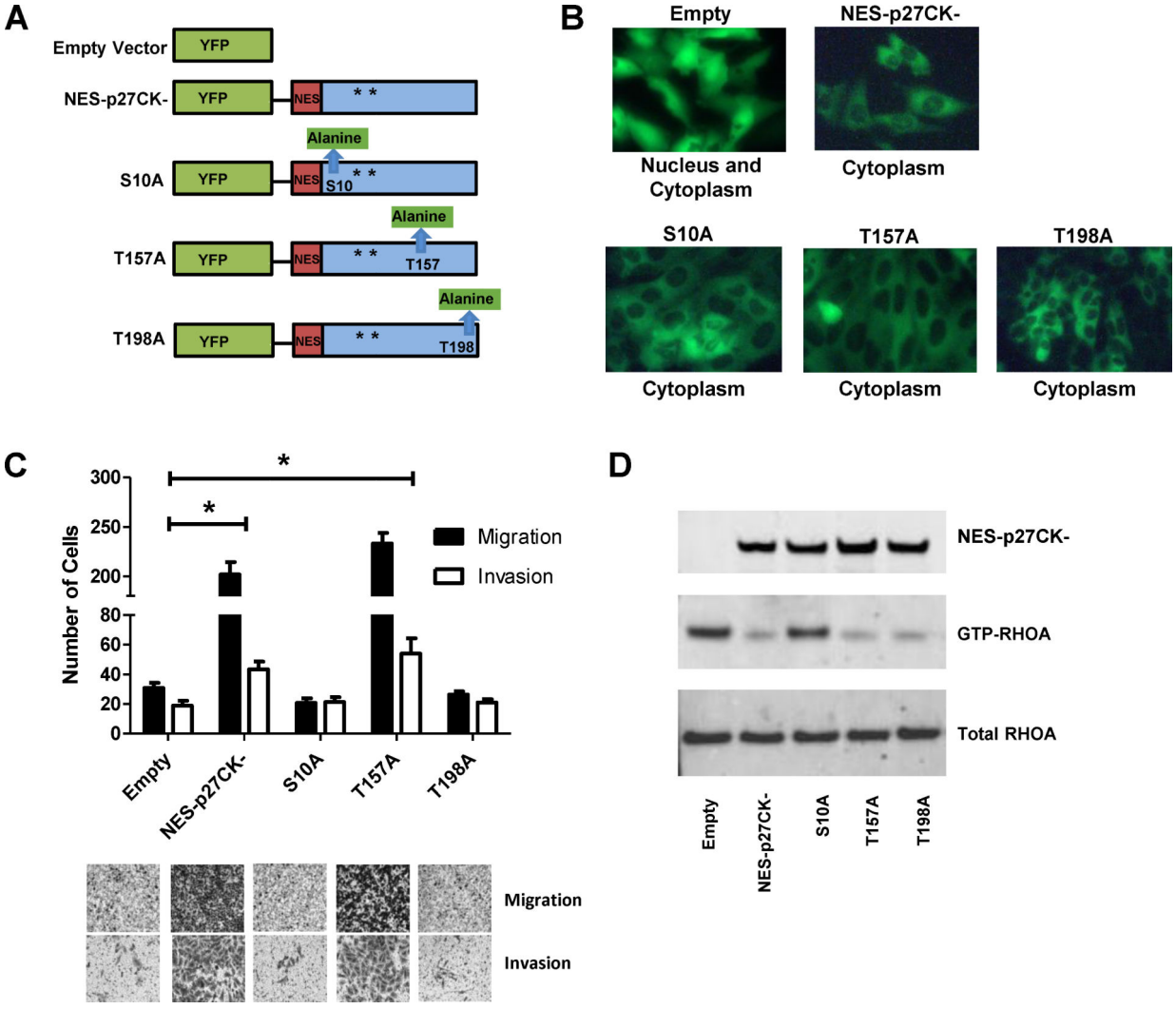

Figure 4.

Functional analysis of cytoplasmic expression of p27 in OS. A: The NES constructs used in this study. All the NES-p27 constructs contain mutations in CDK binding domain (CK-) as indicated by the asterisks. NES and EYFP denote Nuclear Export Sequence and Enhanced Yellow Fluorescent Protein, respectively. The mutations in S10A, T157A and T198A are highlighted green. B: The fluorescent images (40X) indicate the subcellular localization of the empty vector (EYFP), NES-p27CK- and phosphomutant proteins in the stable clones. C: The results of the transwell cell migration and invasion assays indicate that the number of migrated and invaded cells in the NES-p27CK- and T157A cells were significantly higher than those in the empty vector control (*$p < 0.05$), as well as the S10A and T198A mutants. Migrated and invaded cells were quantified by counting stained cells in 3 independent microscopic fields at 6 h and 24 h, respectively. The staining was done with Cell Staining Solution included in the Cell Migration and Invasion Kit. Error bars and asterisks represent standard deviations and statistical significance ($p < 0.05$), respectively. D: The RHOA-GTPase activity assay to indicate the effects of cytoplasmic p27 and phosphomutations on the inhibition of the RHOA activity.

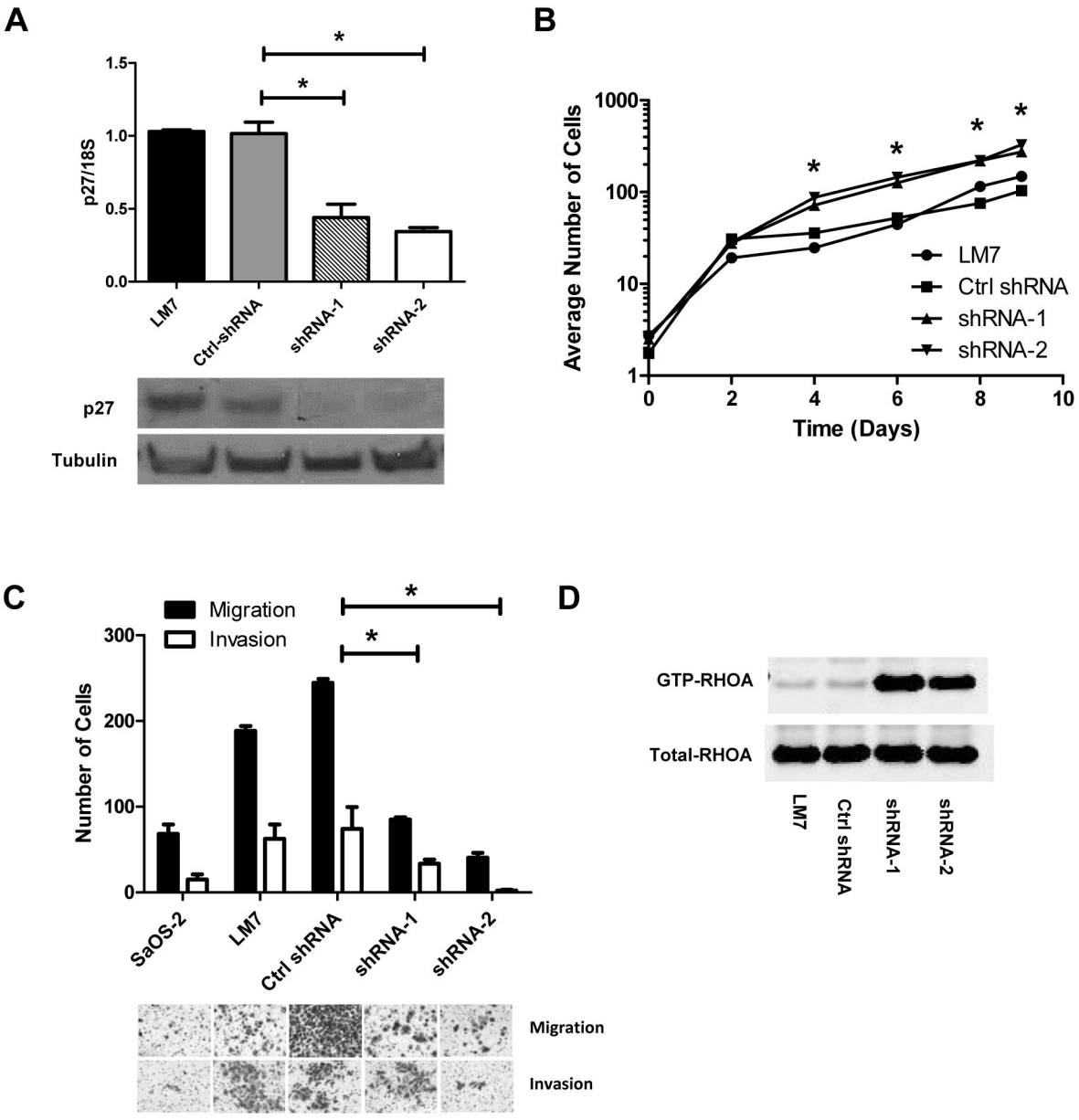

Figure 5.

Functional analysis of shRNA-mediated gene silencing of p27 in OS. A: p27 mRNA (top) and protein (bottom) expressions were measured in LM7 cells alone and with stably transfected Ctrl-shRNA (scramble sequence), p27 shRNA-1 and p27 shRNA-2. The p27 mRNA expression was normalized to 18S ribosomal RNA. B: The growth curves show that p27-shRNA silenced mutants grew faster than the parental and control cells. The plot is in a semi-log scale where X-axis represents days of incubation. Asterisks denote statistical significance when comparing the number of cells in shRNA mutants with LM7 and control cells at each time point (*$p < 0.05$). C: Transwell migration and invasion assays show that the numbers of migrated and invaded cells in the p27-silcenced cells were significantly lower than the control cells. Error bars and asterisks represent standard deviations and

statistical significance (*$p < 0.05$), respectively. D: The RHOA-GTPase activity assay shows that RHOA activation in the p27-silcenced cells was higher than in the parental or control cells.

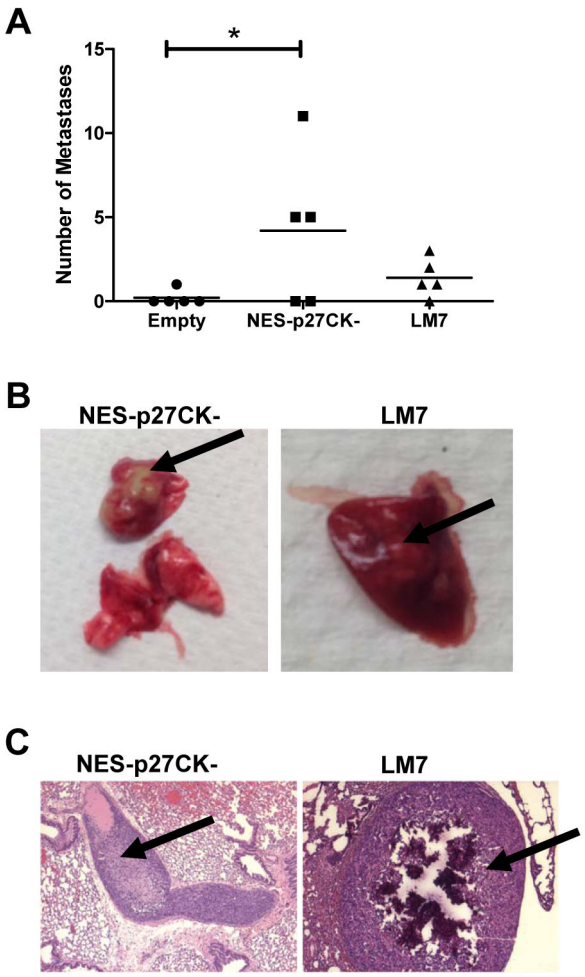

Figure 6.

Cytoplasmic p27 promotes the development of metastasis in an experimental mouse model. A: The number of pulmonary metastases in mice injected with SaOS-2 containing NES-p27CK- was significantly increased when compared to the empty vector control (*$p < 0.05$, one-tailed t-test). The lines in the plot denote the average intensity values of the groups. B: Macroscopic examination of lungs derived from the mice injected with SaOS-2 cells with NES-p27CK- and LM7 cells. C: Histological examination of metastases developed in the lung sections dissected from SaOS-2 cells with NES-p27CK- (left) and LM7 cells (right) and after H&E staining. Arrows indicate the metastatic nodules.